Haukur Ingason

An Experimental Study of Rack Storage Fires

Brandforsk Project 602-971

SP Swedish National Testing and Research Institute
SP Fire Technology
SP REPORT 2001:19

Haukur Ingason

An Experimental Study of Rack Storage Fires

Brandforsk Project 602-971

SP Swedish National Testing and Research Institute
SP Fire Technology
SP REPORT 2001:19

Abstract

This report describes an experimental study of rack storage fires with in-rack sprinklers. Four large-scale tests with Standard Class II commodity, which consists of double triwall corrugated paper cartons, were carried out. Two fast response in-rack sprinkler heads were mounted in the flue at two heights. Measurements of heat release rate, in-rack flame height, excess gas temperature, gas velocity, plume profiles and activation times of the in-rack sprinklers are presented.

Comparison of the measured data against axi-symmetric power law correlations for the in-rack plume flow was carried out.

Key words: Rack storage, heat release rate, in-rack plume, in-rack flame height, in-rack temperature, in-rack velocity, in-rack thermal plume, fire growth rate, in-rack sprinkler

Sveriges Provnings- och Forskningsinstitut
SP Rapport 2001:19
ISBN 91-7848-863-X
ISSN 0284-5172
Borås 2001

Swedish National Testing and Research Institute
SP Report 2001:19

Postal address:
Box 857, S-501 15 BORÅS, Sweden
Telephone + 46 33 16 50 00
Telex 36252 Testing S
Telefax + 46 33 13 55 02

Table of contents

Foreword

On behalf of the Swedish Fire Research Board (BRANDFORSK), SP-Fire Technology has carried out a series of large-scale tests of combustible material in a rack storage type of configuration. The project is a part of a long-term research project series related to fire hazards in large warehouses. Earlier projects have mainly included reduced scale fire tests, whereas the present study is aimed at validating earlier results in this area by performing large-scale tests.

The consultative group for the project consisted of the following:

- Leif Beisland, Folksam, Stockholm
- Kaare Brandsjö, FRC Fire and Rescue Consultant, Stockholm
- Sven Jönsson, IKEA, Älmhult
- Claes Malmqvist, National Board of Civil Defence, Rescue and Fire Services, Karlstad
- Lars Hellsten, Scania, Södertälje
- Conny Nabrink, Projektör AB, Torslanda
- Per Sjölander, AssiDomän Försäkring AB, Stockholm
- Torsten Södergren, if Skadeförsäkring, Malmö
- Ari Santavuori, Sampo Industriförsäkring AB
- Henry Persson, SP Brandteknik
- Magnus Arvidson, SP Brandteknik

I gratefully acknowledge the help of all members of the group.

The author would also like to acknowledge Dr John L. DeRis at Factory Mutual Research Corporation for his contribution to the discussion of fire growth rates (chapter 5.5).

1 Introduction

High rack storages are often protected with in-rack sprinklers inside the longitudinal and transverse flues (gaps). The efficiency of the in-rack sprinkler system depends on the packaging and storage arrangement, as well as on the flammability of the commodity. Other important factors are sprinkler orientation and responsiveness of the heat-sensitive element and the type of water supply e.g. a dry pipe or wet pipe sprinkler system. Any delay in sprinkler activation may be critical for control of the fire. If a significant amount of flame passes a sprinkler before it activates, combustibles at higher levels may easily be ignited, thus reducing the possibility of the sprinkler water to penetrate to the fire seat.

Correlations to predict the activation time of the first in-rack sprinkler are of practical importance. Such prediction is done routinely in simple room configurations using power law correlations of temperature and velocity in plumes and ceiling jets [1, 2, 3]. In order to calculate the activation time for in-rack sprinklers, we need information on flow conditions close to the sprinkler head.

Simple in-rack fire plume correlations, which can be used to predict the flow conditions inside the vertical flues, have previously been presented by Ingason [4, 5]. The correlations provided were mainly based on 1/3 scale model tests with single wall corrugated paper cartons folded inside with single wall corrugated board sheets [6]. Additionally, one large-scale test was performed using Standard Class II commodity. Ingason [4, 5] concluded that there is a great need for further large-scale testing in order to validate these correlations. The present study therefore included four large-scale experiments with Class II commodity in a palletised rack storage, where heat release rate, in-rack gas temperatures, in-rack gas velocities and in-rack flame height was measured for different flue widths. Furthermore, fast response dry pipe sprinklers (no water supply) were mounted in the flues at two different heights in order to measure the activation time.

2 Background

Although numerous large-scale experiments using rack storage fires have been performed throughout the world [7, 8, 9, 10, 11, 12, 13, 14, 15], no information is available on in-rack flow conditions from these tests. The reason is probably that the tests were mainly performed to study the behaviour of sprinkler systems in controlling or suppressing rack storage fires, rather than systematically to study the in-rack plume flow and flame spread. It is therefore difficult to draw conclusions on the effects of different flue (gap) sizes on the flame spread. Recommendations in NFPA 231C [16] (which are based on full-scale experiments carried out at the Factory Mutual Research Test Center, West Clocester, Rhode Island [16]) on the size of flues (nominal size according to NFPA 231C is 152.4 mm) are probably more related to the passage of water in the rack storage than to the effects of flame spread.

The theoretical and experimental work [7, 8, 9, 17] on rack storage fires conducted so far has been concentrated on predicting what occurs above the rack storage and below the ceiling, rather than what occurs inside the store. The work on in-rack plume flows done by the author [4, 5, 6, 19] is mainly based on reduced-scale tests. The author of this report has pointed out earlier the need for more support from large-scale testing [5].

Thomas [18] studied some large-scale fire test performed in the United Kingdom [10, 11], and found no data on heat release rates or mass loss rates for rack storage fires. Flue ignition resulted in the most rapid fire propagation, and it was observed that the flame propagation was rapid enough to involve boxes on the upper levels before the box contents became involved [10]. With flue ignition, an increase in box spacing from 75 mm to 150 mm resulted in a reduction in the time taken for the flame to reach the top of the rack storage. However, the ignition source was not identical for these two flue widths (being larger for the 150 mm flue), which may have affected the initial fire spread. Based on his investigation of the UK tests, Thomas [18] suggested that there is probably a gap size with a highest spread rate, that there is evidence that the width of the vertical gap affects average upward flame speed and that the average flame speed is of the order of 0.1 m/s.

Field [10] gives a thorough description of a series of large-scale tests carried out in the United Kingdom. Protection of the storages by a conventional in-rack system incorporating 68 °C glass bulb sprinkler heads was investigated and found to be unsatisfactory. Flames tended to pass a given sprinkler location before it operated, and subsequently ignited combustibles at a higher level. Sprinkler heads that were capable of operating at an earlier stage in the fire development were therefore tested in a new series of tests. Fast-responding sprinkler heads were expected to control a fire whilst it was still in its early stages of development. The sprinklers were located at the junction of the transverse and longitudinal flues. In addition, the spacing between the boxes, i.e. dimensions of the transverse and longitudinal flues, was also varied. The results can be summarised as follows:

- in order to operate ahead of an approaching flame, a sprinkler head must have an adequately high sensitivity,

- the glass bulb sprinklers located at all but the highest levels in the rack generally operated after the flame had passed (see Figure 1),

- the intermediate response solder-cup sprinkler used was significantly more sensitive than the glass bulb type; frequently, although not exclusively, operating before the flame had passed (see Figure 1),

- the fast response solder-link sprinkler consistently operated ahead of the flame (see Figure 1),

- fires ignited within the flue developed rapidly, frequently reaching the top of the rack within two minutes. The flame propagation was rapid enough to involve boxes on the upper levels before the box contents (wood wool and polystyrene chips in cardboard boxes) became involved. Lateral flame spread at this stage was reported to be minimal,

- fires ignited on the face of boxes initially developed slowly, taking about seven minutes to ignite boxes on the second level. This appeared to be a critical point in the fire's development. After this critical stage, flames tended to move preferentially towards the central flue, and the fire subsequently behaved as if it had been ignited in the flue,

- an increase in box spacing, i.e. the dimension of transverse and longitudinal flues, resulted in a decrease in the time taken for the flame to reach the top of the rack for flue ignition.

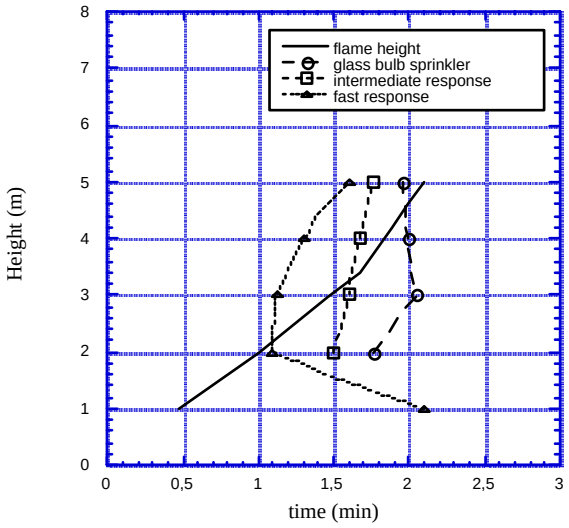

Figure 1 Typical sprinkler response to a fire ignited in the vertical flue (based on information given in reference [10]).

The simple in-rack correlations provided by Ingason [4, 5], i.e. excess centreline gas temperature and velocity, could be used to predict the response times given in Figure 1 (at least the first sprinkler). Unfortunately, no information about heat release rate as a function of time is available for these large-scale tests.

The observation that the wider flues (150 mm instead of 75 mm) tended to decrease the time for the flames to reach the top is very interesting. The model scale tests presented in [4] show contradictory results. A possible explanation is that the change in spacing from 75 mm to 150 mm was, according to Thomas [18], accompanied by a more powerful ignition procedure. It is known from the model scale tests [4] that increasing the size of the ignition source will shorten the time for the flames (from ignition) to reach the top of the rack storage. The slope of the heat release rate curve, however, was not affected.

Ingason and De Ris [19] investigated the effects of flue space for storage geometries using four steel towers and a gas burner. The steel towers represented an idealisation of a rack storage configuration at reduced scale. Each tower was 1.8 m high and 0.3 m x 0.3 m wide. The fuel was supplied from a circular gas burner at the floor. Three different gaseous fuels were used: carbon monoxide (CO), propane (C_3H_8), and propylene (C_3H_6). These fuels covered a wide range of flame sootiness, resulting in distinctly different flame heat fluxes. The incident radiation to the walls was found to be dependent on the HRR, the soot point of the fuel [20] and the distance between the parallel towers used in the study.

Alvares et al. [24] found that the effects of distance between the parallel cardboard panels were of importance in their study, and they incorporated these effects in a correlation for the mass loss rate.

The in-rack plume correlations presented by Ingason [4, 5, 6, 19] include the effects of the vertical flue width. This effect appears to be important but needs to be validated by more large-scale testing.

3 Theoretical aspects

Ingason [6] presented a quasi-steady state fire plume law for in-rack centreline gas temperature, gas velocity and flame height derived from a simple physical model. This exploratory theoretical model suggested that the excess in-rack centreline gas temperature should be proportional to the instantaneous convective heat release rate, $Q_c^{2/3}$ and be inversely proportional to height, z. The in-rack gas velocity should be proportional to $Q_c^{1/3}$ and be independent of z. The flue width (w) dependence was also included in the correlations. The relations have the same functional form as a convective plume flow above a line fire source [21].

A plot of the measured temperature in the two different scales appeared to give a reasonable good correlation [6]. The scatter was, however, substantial. In order to obtain similar correspondence for the velocity in the two scales, it was necessary to use Froude number scaling with storage height as the length scale. This does not comply with the results of a linear plume model, which indicates constant velocity independent of height z. Hence, in order to investigate whether other sets of correlations would improve the results, the experimental data was plotted using axi-symmetric fire plume laws [5]. The axi-symmetric correlations yielded considerably less scatter for the large-scale test performed. This indicated that the experimental data obeys axi-symmetric power laws better than the linear plume power laws as suggested by the linear plume model given in reference [6]. Plotting the available flame height data indicated the same tendency.

For axi-symmetric power law correlations, the flame height should be proportional to the chemical heat release rate, $Q^{2/5}$, and the excess centreline gas temperature should be proportional to the instantaneous convective heat release rate, $Q_c^{2/3}$ and inversely proportional to $z^{5/3}$. The centreline gas velocity should be proportional to $Q_c^{1/3}$ and inversely proportional to $z^{1/3}$.

3.1 In-rack plume flow correlations

Ingason [4, 5] plotted the in-rack flame height data for the experiments with corrugated paper cartons on two different scales (1:3 and 1:1) using axi-symmetric power law correlations.

The flame height data was obtained from video recordings by comparing the ‘average’ fluctuation of the flame tip against a scale painted on the boxes. A least squares fit to the in-rack flame height data (model scale tests and one large-scale test) yielded the following equation [4, 5]:

$$L_f = -3.73w + 0.343Q^{2/5} \qquad (1)$$

where w is the vertical flue width in metre and Q is the total heat release rate in kW. Equation (1) is valid for $L_f \leq H$. The flue widths (w) were 50, 75 and 100 mm in 1:3 scale and 150 mm in 1:1 scale. Similar correlation was given by Ingason and De Ris [19] for the steel tower tests (w=63, 82, 100 and 150 mm). Ingason [4, 5] also presented correlations for in-rack excess centreline temperature and velocity. The excess temperature is given by equation (2):

$$\Delta T_0 = 28\left[\frac{T_\infty}{g c_p^{\,2}\rho_\infty^{\,2}}\right]^{1/3}\frac{Q_c^{\,2/3}}{(z-z_0)^{5/3}} \qquad (2)$$

where Q_c is the convective heat release rate in kW. C_p= 1.01 kJ/kg K, 284 K, kg/m^3 and g=9.81 m/s^2 were used to determine the non-dimensional constant, C_T=28. The equation was found to be valid for $(z-z_0)/Q_c^{2/5}$ >0.20. At $(z-z_0)/Q_c^{2/5}$ <0.20 the average excess centreline temperature (ΔT) was found to be equal to 836 K. The virtual source was found to obey the following relation [4, 5]:

$$z_0 = -3.73w + 0.083Q^{2/5} \qquad (3)$$

Ingason [4] used the Froude scaling law to plot the velocity data. Fitting a curve (least squares) to the large-scale test for $Q_c^{\,1/3}/(z-z_0)^{1/3}$<3.4 yielded the following equation:

$$u = 3.54\left[\frac{g}{c_p\rho_\infty T_\infty}\right]^{1/3}\left(\frac{Q_c}{(z-z_0)}\right)^{0.45} \qquad (4)$$

where the same ambient conditions as earlier were used.

The traditional way to define a thermal plume width, $\boldsymbol{b}_{\Delta T}$, is by means of the width at the point where the temperature rise has declined to $1/2\,\Delta\boldsymbol{T}_0$. Here, T_0 is the plume centreline temperature and the width is measured from the flue centre-line. Measurements were carried out in the tests presented here in order to obtain a correlation for the in-rack thermal plume. Ingason and De Ris [19] presented a correlation for the thermal plume width, $\boldsymbol{b}_{\Delta T}$, based on their experiments using four steel towers.

$$\frac{b_{\Delta T}}{L_f^{\,1.1}} = 0.177\frac{z}{L_f} \qquad (5)$$

where L_f is calculated from equation (7) in reference [19]. Actually equation (1) in this report can be used to calculate L_f since the difference is relatively small.

As mentioned in Chapters 1 and 2, Ingason [5] pointed out that these correlations need further validation by performing additional large-scale tests with varying flue widths. These additional tests are presented here, and the experimental results were used to compare the data with equations (1)-(5): see chapter 4.

3.2 Heat release rate (HRR)

There are several studies available, which have relevance to heat release rate (HRR) in rack storage fires. An overview of these studies is given below, categorized in accordance with the mathematical representation of the HRRs.

Power law correlations

Yu and Stavriandidis [9] presented a correlation showing that the initial convective HRR per tier height correlated with a power-law dependence on time to the third power (t^3). The convective HRR per tier is given by the following equation:

$$Q_c = \alpha(t - t_0)^3 \qquad (6)$$

where Q_c is the convective HRR in kW, α is a fire growth coefficient (kW/s^3), t is the time in sec and t_0 is the incipient time of fire growth (s). A data fit yielded α = 0.0448 kW/s^3 per tier. This function worked well for the initial fire growth rate period, i.e., convective heat release rates up to 800 kW per tier, which corresponds to 3200 kW for the four-tier large-scale test presented here. The fire growth rate coefficient α in Yu and Stavriandidis [9] correlation for four-tier high rack storage is 0.179 kW/s^3 (4 x 0.0448). The purpose of the study was to develop mathematical correlations for the transient ceiling flow in the period when the convective HRR had a power-law dependence on time to the third power. The fuel used in the study consisted of polystyrene cups packaged in compartmented, single-wall corrugated paper cartons. Eight cartons were placed on a wood pallet, forming a stack of two cartons wide by two cartons deep by two cartons high, defined as a pallet load. The fuel array was two-pallet loads wide, two-pallet loads deep and two, three, four and five tiers high (the number of tiers is equal to the number of pallet levels). The experimental data coincided on a single curve when the convective HRR per tier was plotted as a function of the time, $t-t_0$. No physical explanation to why the experimental data coincided on a single curve for the different tiers was given.

MacGrattan et al. [22] presented an HRR correlation which was intended to approximate the estimated growth rate of the cartoned plastic commodity burns conducted at FMRC. The HRR correlates with a power-law dependence on time to the second power (t^2). The fire growth rate coefficient was 1.77 kW/s^2. A heptan spray was used to simulate the HRR. The HRR was intended to approximate the estimated growth rate of the cartoned plastic commodity burns conducted at FMRC [23].

Exponential correlations

Thomas [18] studied large-scale fire tests performed in the United Kingdom [10,11]. He found no data on HRR or mass loss rates, but he was able to analyse temperature and flame height data. Based on that, he argued that the fire growth rate of rack storage fires with line ignition could be described with an exponential function. He was able to estimate the doubling time of 10 – 20 seconds. This means that the HRR doubles in size every 10 – 20 seconds. This time is constant for the exponential model.

Alvares et al. [24] presented fire growth rate correlation for parallel panels of heavy-grade cardboard, simulating stacked boxes. The panels used measured 1.2 m wide, 1.8 m high and were spaced from 0.05 m to 0.33 m apart, in 0.05 m

increments. A small ignition source was placed centrally 0.3 m from the bottom of each panel. Data from the experiments was correlated in terms of formulas derived from theoretical analysis of upward flame spread and vertical mass burning. Alvares et al [24] developed a simple exponential correlation for the mass loss rate, which correlated well with their data on parallel cardboard panels. Their expression was derived from basic flame spread correlations:

$$\dot{m} = m_0 b e^{b(t-2t_0)} \qquad (7)$$

with b=4.1/d+0.013 and d is distance between parallel walls. The HRR can be obtained by multiplying the mass loss rate in eqn. (7) with the heat of combustion of the combustible material.

Ingason [6] found that the initial convective HRR was better described by an exponential function rather than a power-law dependence on time to the third power, as given by Yu and Stavriandidis [9]. Ingason's [6] finding was based on one large-scale test with four-tier high rack storage loaded with double triwall corrugated paper cartons (Standard Class II commodity):

$$\Delta Q_c = 2.27 e^{0.102(t-t_0)} \qquad (8)$$

where $\Delta Q_c = Q_c - Q_{c,0}$, and $Q_{c,0}$ is the convective heat release rate at t_0. Here, the incipient time, t_0, was defined as the time when the convective HRR started to increase notably in size. This time was obtained by investigating the measured convective HRR and by observing the initial flame heights from video recordings. The time t_0 agreed well with the time when the mean flame height of the ignition source just started to increase in size.

Based on simple flame spread modelling of the vertical surface of the commodity above the ignition sources, Ingason [25] presented another type of mathematical representation of the convective HRR for rack storage fires. Based on the results from an analysis of experimental data found in SP's database, Ingason [25] found that the following type of mathematical expression could represent the initial convective HRR:

$$Q_c = H \alpha e^{\beta t} (a + bt) \qquad (9)$$

where the parameters α, β, a and b can be determined from experimental data. H is the total geometrical height of the store. The experimental data used in the analysis is presented in figure 2. The fuel array was two-pallet loads wide, two-pallet loads deep and two, three, four and five tiers high. The ignition source was a standardised one, i.e. four separate ignition sources symmetrically placed at the centre flue space of the fuel array and at the bottom of each carton at the lowest tier. Equation (9) should be used with caution for a higher convective HRR than 7 MW: the fire does not necessarily develop in the same way for higher HRRs. The data used to derive equation (9) was obtained from experiments conducted under a hood system with a maximum capacity of 10 MW chemical HRR.

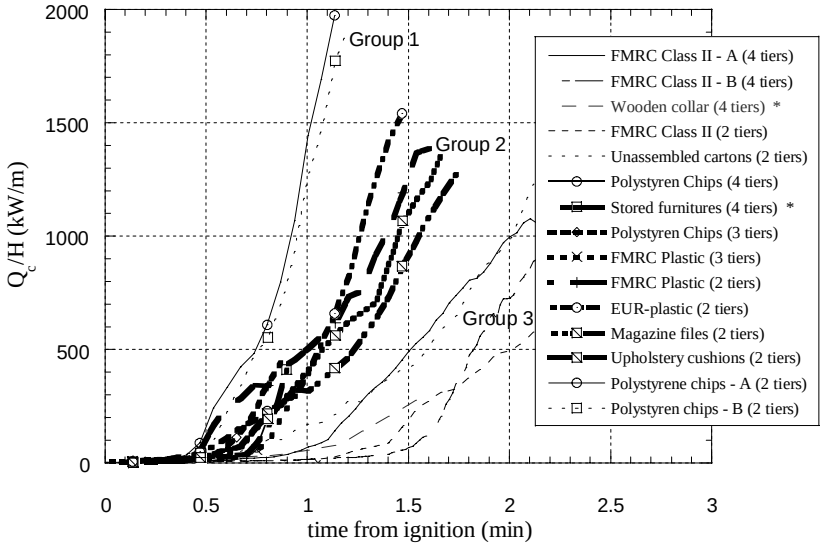

Figure 2 The convective HRR (Q_c) per height of the rack (H) as a function of time. The different groups of fire growth rates are indicated in the plot.

Figure 2 indicates three distinct groups of fire growth rates. A fast fire growth rate (Group 1) (α = 1.41 kW/m^2, β = 0.036 s^{-1}, a=0.4 m and b= 1.57 m/s; R=0.99), an intermediate fire growth rate (Group 2) (α = 0.65, β = 0.015, a=0.4 and b= 4.5 ; R=0.94) and a relatively slow fire growth rate (Group 3) (α =0.36 , β =0.024, a=0.4 and b=0.99 ; R=0.93). The negative value of a obtained by curve fit in reference [25] is not physically justified. Therefore, we assume a equal to 0.4 m which corresponds to the width of the initial pyrolysis zone created by the four ignitions sources. The derivation of the fire growth constants α, β, and b by curve fitting is based on time in seconds. R is the linear correlation coefficient obtained from the curve fit procedure. Group 1 include polystyrene chips in paper cartons, group 2 includes mainly plastic commodity in and without paper cartons, and group 3 includes natural materials such as cartons with thick walls and wood. No consideration was given to the incipient time, t_0, in the analysis. A general description of the commodities presented in figure 2 is given below:

Wooden Collar: Spare parts for cars consisting of expanded and unexpanded plastic items stored on a wood pallet with pallet rims of wood (wood collar), but without any cover on the top and a perforated fibreboard sheet at the bottom. The pallets were stored in a rack storage, five tiers high, corresponding to a storage height of 6.5 m.

Polystyrene chips stored in single wall corrugated paper cartons on wood pallets.

FMRC Class II: A Standard Class II commodity consists of double triwall corrugated paper cartons. The double cartons are folded onto a sheet-metal liner and then placed on a wood pallet.

Magazine files and letter trays made of polystyrene, stored in paper cartons on wood pallets. Each test consisted of three types of pallet load and in all three tests these were mixed in order to get as equal composition as possible.

FMRC Standard Plastic commodity on US wood pallets. The commodity consists of single-wall corrugated cartons containing 125 polystyrene cups.

"EUR Plastic" : a repacked version of the FMRC Standard Plastic commodity, in order to obtain cartons which fit to the European pallet system, 1200x800 mm. Original FMRC material was used, except for the paper carton.

Upholstery Cushions stored in paper cartons on wood pallets. Each test consisted of three types of pallet load, and in both tests these were mixed in order to get as equal composition as possible.

3.3 Response time of in-rack sprinkler

Usually, in-rack sprinkler heads are aligned with the upward flue flow (pendent) and the deflector is headed into the plume flow. The sprinkler deflector of a pendent in-rack sprinkler may delay the activation of the sprinkler by blocking the free stream around the glass bulb (wind shadow effects). Wind shadow effects on sprinkler activation are discussed by Ingason [4,26]. Normally, the wind shadow effects are created by the yoke arms of the sprinkler, which in turn is dependent on the orientation of the yoke arms in relation to the free stream flow. The RTI theory [27] for calculating the time to activation of sprinklers was shown by Ingason and Persson [26] to be valid irrespective of the orientation of the sprinkler.

Weak evidence for the conjecture that the theory may also be valid for the in-rack sprinkler situation can be obtained from the work by Heskestad and Bill [28]. They present measurements of a glass bulb sprinkler (N) showing similar RTI values obtained either with the yoke arms aligned parallel with the flow or when the deflector is headed into the flow. When the sprinkler yoke arms are aligned perpendicular to the flow, the RTI value is about two times less than in the two other situations. These results indicate that the deflector, which may explain the increase in the RTI value, blocks the glass bulb.

The temperature rise of the bulb of the in-rack sprinkler can be obtained with the following equation [28]:

$$\frac{d(\Delta T_e)}{dt} = \frac{\sqrt{u}}{RTI}(\Delta T_g - \Delta T_e) \qquad (10)$$

where ΔT_e is the excess temperature of the sensing element and ΔT_g is the excess gas temperature in ^{o}C. Hence, given the RTI, together with ΔT_g(t) and u(t) from equations (2)-(4), the thermal response ΔT_e(t) can be obtained using numerical methods. The activation is usually at ΔT_e(t=t_{op})=68 ^{o}C.

4 Experimental Set-up

Four large-scale experiments were carried out under the Industry Calorimeter [29] in SP's fire hall. The calorimeter, which is of same type as the FMRC Fire Products Collector [30], can measure up to 10 MW chemical HRR. Both the convective and the chemical HRR were measured. A Standard Class II commodity was used, which consists of double triwall corrugated paper cartons (each 12 mm thick). The double cartons were folded onto a sheet-metal liner and then placed directly onto the rack storage beams. No wood pallets were used. The outer dimensions of each carton were 0.8 m x 1.2 m x 1.0 m and the moisture content was 8 % by weight.

Figure 3 A large-scale experiment with Standard Class II material under the Industry Calorimeter at SP.

A double-row steel rack was used to hold the commodity. The widths of the vertical flues (w) were 75, 150, 225 and 300 mm. The height of the horizontal flues was 300 mm. The total height of the rack storage was 5.2 m. Figure 3 shows that the four ignition sources were symmetrically placed as close as possible to the centre flue space of the fuel array, at the bottom of each carton at the lowest tier. The ignition source consisted of insulating fibreboard (similar to cellucotton rolls),

75 mm in diameter and 75 mm long, each soaked with 120 ml heptane and wrapped in a polyethylene bag. The mean flame height of the ignition source was about 0.9 m measured from the bottom of the carton.

Centreline in-rack temperatures and velocities were measured at four elevations: z = 0.97 m, 2.27 m, 3.57 m and 4.87 m. Each of these positions corresponds to 2/3 of the height of the carton. The ambient indoor temperature varied between 19 and 21 °C.

4.1 Instruments

A total of 34 thermocouples were used to measure plume temperatures at four elevations. The in-rack temperatures were measured with welded type K thermocouples (Chromel-Alumel), with a wire diameter of 0.25 mm. The gas velocity was measured with bi-directional pressure differential flow probes (D=16 mm and L=32 mm) [31] at four different elevations. The thermocouples were attached to each bi-directional probe close to the sensor head. Figure 4 shows the positions of thermocouples and bi-directional probes. Horizontal thermocouple piles (supported on a steel rod) were mounted in the **x** and **y** directions at **z**=2.27 m, 3.57 m and 4.87 m (see fig 4). Thermocouples at height z=2.27 m were positioned at x=-0.3, 0, 0.15, 0.3, 0.5 and 0.7 m and at y=-0.3, 0, 0.15, 0.3, 0.5 and 0.7 m. Thermocouples at height z=3.57 m were positioned at x=0, 0.3, 0.7 m and 1.2 m and at y=0, 0.3 and 0.7 m. Thermocouples at height z=4.87 m were positioned at x=-0.7, -0.3, 0, 0.15, 0.3, 0.5, 0.7, 1.0 and 1.3 m and y=-0.5, -0.3, 0, 0.15, 0.3, 0.5 and 0.7 m.

No corrections due to radiation effects on the thermocouple measurements were carried out in this study. The velocity was not corrected for variation in the Reynolds number according to calibration curves reported in [31]. The data was recorded by a data acquisition system every other second.

The flame height data was obtained from video recordings by comparing the ‘average’ fluctuation of the flame tip against a scale painted on the boxes. This method, although subjective, was found to be reasonably accurate (+/- 50 mm by estimation), as the fluctuations of the flames were substantially less than those observed in free axi-symmetric plumes. A more objective method would be to define the flame height as a mean temperature, but that would require either significantly more instrumentation or more comprehensive analysis. However, for the purpose of the present study, the method used here is considered satisfactory.

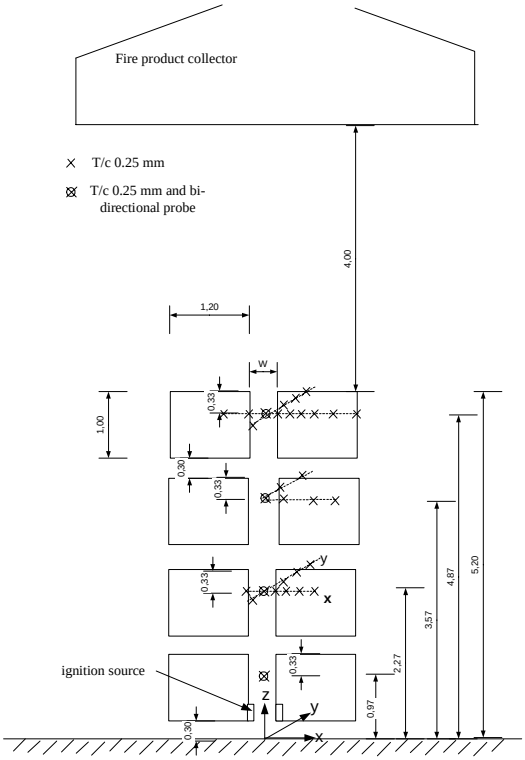

Figure 4 The experimental set-up and position of instrumentation (thermocouples and bi-directional pressure differential flow probes). Horizontal thermocouple piles were mounted in the x and y direction at z=2.27 m, 3.57 m and 4.87 m.

4.2 In-rack sprinkler

The in-rack sprinkler was of type Wormald A, Standard Spray Sprinkler (SSP) with a RTI value of 35 $m^{1/2}s^{1/2}$ (for standard orientation). Two sprinklers were mounted (pendent position i.e. with the deflector plate directed perpendicular to the in-rack plume flow. The lower sprinkler was mounted at z=2.27 m (position of deflector) and the higher one at z= 4.87 m. Each sprinkler was placed as close as possible (50 mm) to the instruments in pendent position. The sprinkler was not connected to a water supply system. The sprinkler was, however, attached to a 13 mm diameter pipe with 100 mm water column in order to register the activation of the sprinkler. When the sprinkler activated water splashed and consequently it was possible to register the activation time.

Tests were performed in a wind tunnel [32] with the sprinkler deflector orientated perpendicular to the air stream (pendent position). The glass bulb was shielded from the free air flow and an activation delay was generated. This problem has been thoroughly discussed by Ingason [26]. Three tests were done with a gas velocity of 1.75 m/s and 135 ^{o}C gas temperature. The activation times were 71, 74 and 62 seconds. In the standard position, with the yoke arms perpendicular to the air flow (standard position), the activation time was 20 seconds. The calculated RTI value according to ISO 6182 was 158 $m^{1/2}s^{1/2}$ in pendent position (worst orientation) and 35 $m^{1/2}s^{1/2}$ in standard position (best orientation). The RTI value can be used to calculate the response time of the in-rack sprinklers and compare it with the results obtained from the experiments.

5 Data Analysis and Results

This section presents a comparison of the results obtained in the present study and in earlier studies carried out by Ingason [4, 5, 19]. Parameters to be analysed are the in-rack flame height, in-rack gas temperature, in-rack gas velocity, in-rack thermal plume width, heat release rate and in-rack sprinkler activation time. The ratio of the chemical and convective HRR has also been analysed from the experimental data.

5.1 In-rack flame height

The flame height data for the four large-scale tests are plotted in figure 5. Equation (1) is plotted for comparison.

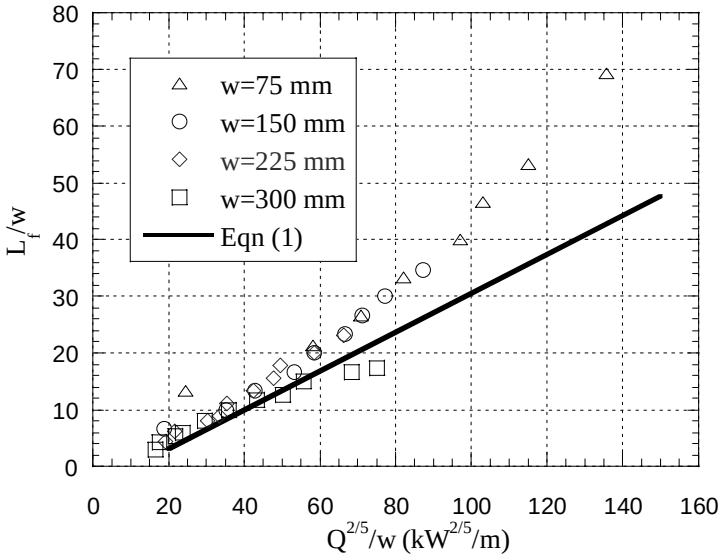

Figure 5 The non-dimensional flame height (L_f/w) plotted as a function of $Q^{2/5}/w$ for the large-scale tests. Equation (1) is based on earlier tests using model scale tests and one large-scale test. W is the flue width.

As can be seen, the agreement between equation (1) and the experimental data is fairly good below $Q^{2/5}/w<60$. However, the slope of the experimental data tends to be considerably steeper than equation (1) for $Q^{2/5}/w>65$. There is also some divergence for the widest flue width, w=300 mm, for $Q^{2/5}/w>60$. The flame height for w=300 mm appears to correspond more to the flame height of a free axi-symmetric fire plume (pool fire). The divergence for smaller flues at $Q^{2/5}/w>60$ is probably due to limited access to entrained air as Q increases, as a result of which the flames tend to stretch upwards.

Generally, there appears to be a lower and upper limit of the flue width for equation (1). These results obtained here indicate that there is a need for a more rational correlation than equation (1) fully to describe the flame height inside the rack storages tested.

5.2 In-rack excess centreline gas temperature

The in-rack excess centreline temperature, ΔT, was plotted at elevations z=2.27 m, 3.57 m and 4.87 m. This corresponds to tier numbers two, three and four. Ingason [5] had noticed earlier that the lowest tier does not behave as axi-symmetric fire plume and thus must be treated separately.

The plot in figure 6 shows that the temperature data follows the –5/3 power of the abscissa, in accordance with the axi-symmetric plume law for temperature, for $(z-z_0)/Q_c^{2/5} < 0.3$ m/kW$^{2/5}$. There is a tendency for the smaller flue widths to yield higher excess temperatures compared with wider flue spaces. Further analysis is needed to improve the correspondence between the experimental data and the influences of w. The representation of the virtual source, equation (3), probably needs to be improved. Figure 7 shows a similar plot for the temperatures measured at the lowest tier.

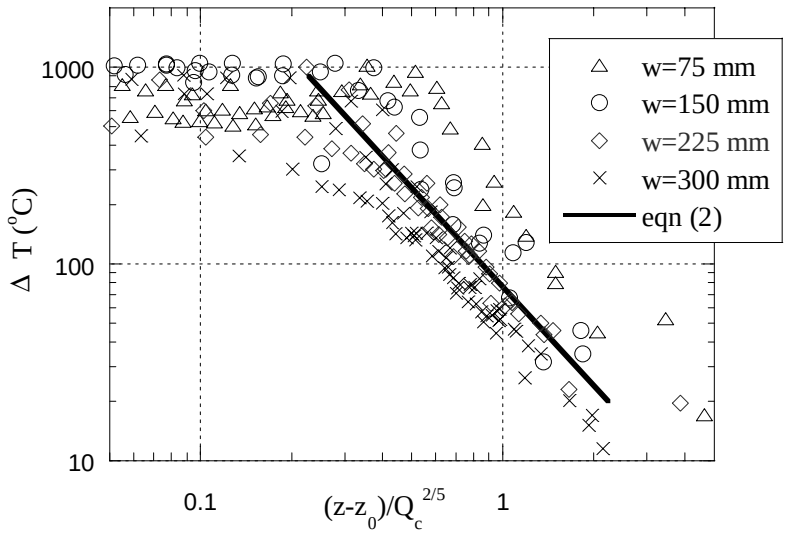

Figure 6 The excess centreline temperature versus $(z-z_0)/Q_c^{2/5}$ for different flue widths, w. The temperatures were measured at tiers two, three and four. The solid line is equation (2). Equation (3) was used to calculate z_0.

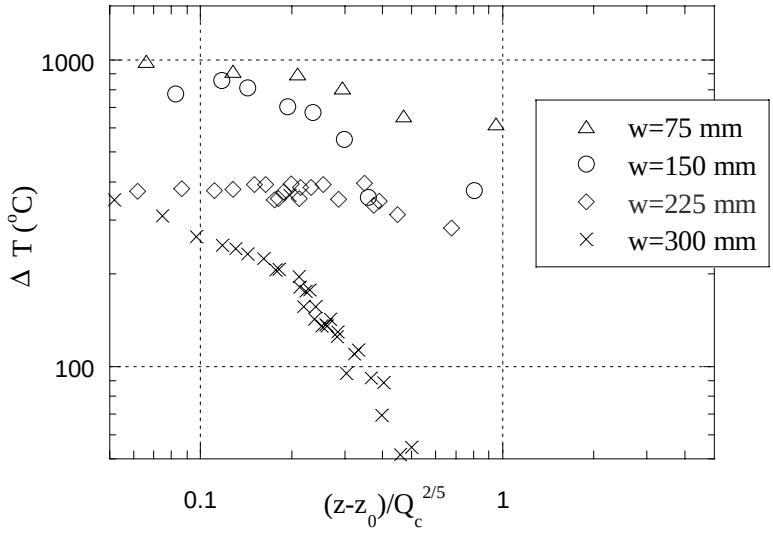

Figure 7 The excess centreline temperature at lowest tier (z=0.97 m) versus $(z-z_0)/Q_c^{2/5}$ for four different flue widths, w. Equation (3) was used to calculate z_0.

The temperature at the lowest tier appears to be relatively constant, i.e. independent of the heat release rate. It is, however, highly dependent on the flue width, w. Narrower flues tend to yield higher temperatures than do wider flue spaces. There is a sharp drop of in the excess gas temperature for the widest flue width, w=300 mm, for $(z-z_0)/Q_c^{2/5} > 0.2$. The reason for this behaviour is probably due to the influence of the ignition source on the measuring results.

5.3 In-rack centreline gas velocity

The in-rack centreline gas velocity was plotted at elevations z=2.27 m, 3.57 m and 4.87 m, and the results compared with equation (4). Figure 8 shows the velocity plotted for all four different flue widths. Equation (3) was used to calculate z_0. The scatter in the data is quite high, but there is a weak trend following equation (4) for $Q_c^{1/3}/(z-z_0)^{1/3} < 3$ $kW^{1/3}/m^{1/3}$. There is a tendency for the smaller flue widths to yield higher centreline velocity than do wider flue spaces. These results are in line with the one obtained for the centreline in-rack temperature, i.e. the correlations do not represent fully the behaviour of the flue width, w, on the measured data.

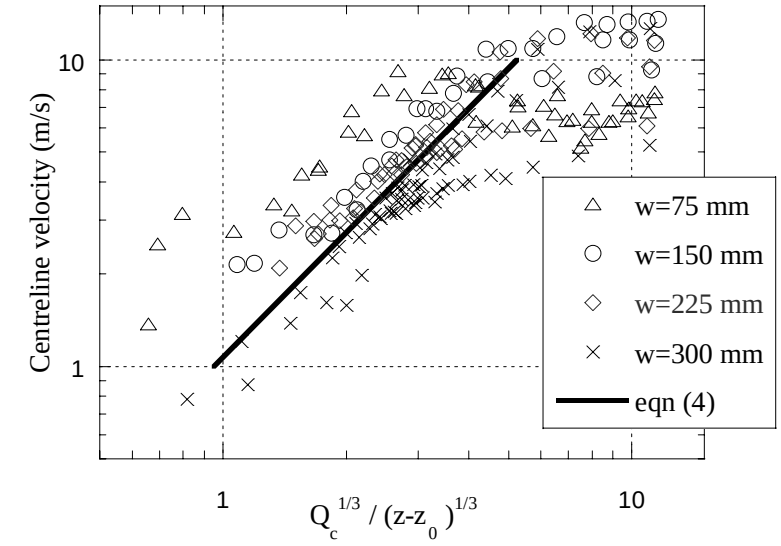

Figure 8 The in-rack centreline velocity as a function of $Q_c^{1/3} / (z - z_0)^{1/3}$ for the four different flue widths, w, and tiers two to four.

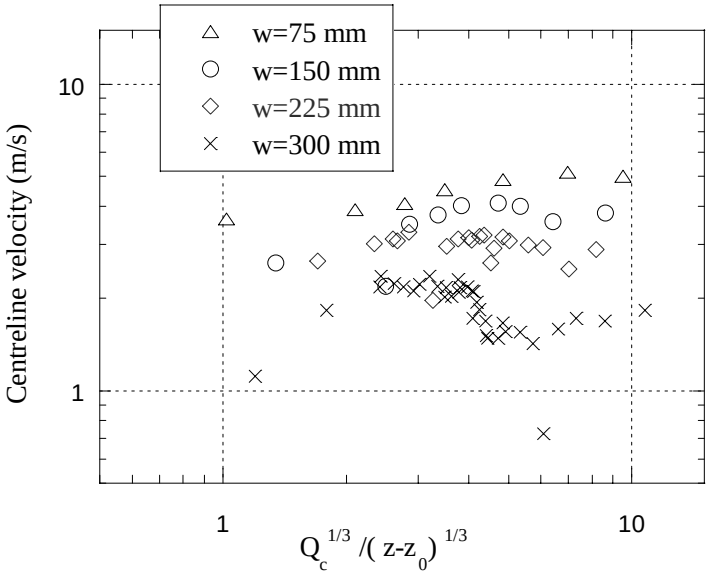

Figure 9 The in-rack centreline velocity as a function of $Q_c^{1/3} / (z - z_0)^{1/3}$ for the four different flue widths, w, and the lowest tier (z=0.97 m).

Figure 9 shows a similar plot for the centreline velocity measured at the lowest tier. The velocity appears to be independent of the heat release rate at this elevation. The velocity is higher for narrower flue widths compared to wider flue widths. The reason for this behaviour is probably due to the influence of the ignition source on the measured results.

5.4 In-rack thermal plume width

The traditional way to define a thermal plume width, $b_{\Delta T}$, is the width at the point where the temperature rise has declined to $1/2\,\Delta T_0$. Here, T_0 is the plume centreline temperature and the width is measured from the flue centre-line. Measurements were carried out in the tests presented here in order to obtain a correlation for the in-rack thermal plume.

The in-rack excess temperature was measured at three different heights. Figure 10 shows the in-rack excess gas temperature, normalised to the centreline temperature and plotted as a function of $x/(z-z_0)\,Q^{0.12}$ for four different flue widths. This was a trial and error procedure, where we found the best correspondence for the data when using $x/(z-z_0)\,Q^{0.12}$. The variables used were originally derived from equation (5) assuming that $b_{\Delta T}$ is associated with x, L_f is proportional to Q and z_0 is associated with z. The results became somewhat different than obtained with equation (5) as will be shown later on. If we assume a Gaussian type of distribution, we can use curve fit procedure to obtain the following equation for the experimental data (linear correlation coefficient, R=0.947):

$$\frac{\Delta T}{\Delta T_0} = 0.996 e^{\left(-31 Q^{0.24}\left(\frac{x}{(z-z_0)}\right)^2\right)} \qquad (11)$$

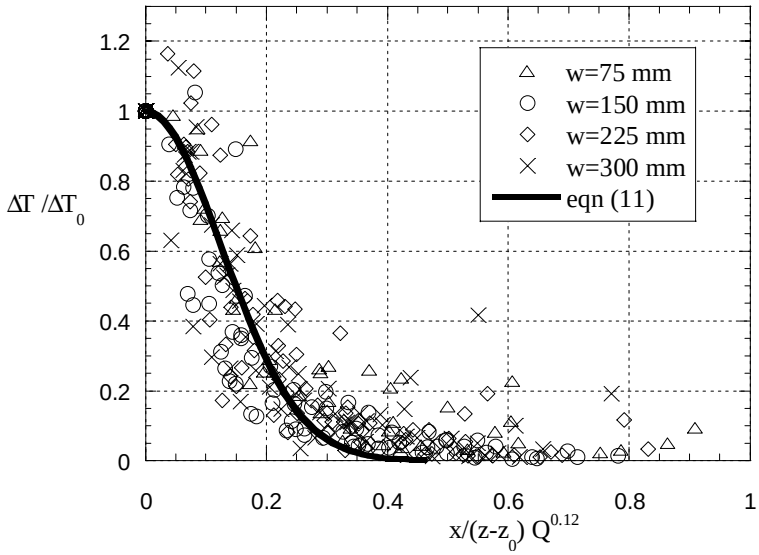

Figure 10 The in-rack excess gas temperature profile measured at three different elevations and for four different flue widths (x-axis). Equation (11) is plotted for comparison. The data was plotted for Q<1100 kW.

The symmetry along the x –axis ($x<0$ and $x \geq 0$) was found to be satisfactory (max occurred at x=0 in most cases) whereas the symmetry along the y-axis was poorer (max occurred at y=0.15 m in most cases). This indicates that the fire was not

entirely symmetrical within the storage. A plot of shifted data points by 0.15 m for $y \geq 0$ was found to correspond well to the x-axis data points. This indicate the shape of the profile is comparable in the x and y flues.

Now we will compare equation (5) and equation (11). If we calculate $b_{\Delta T}$ for a case with Q=500 kW, w=150 mm, z=3.57 m we obtain $b_{\Delta T}$ =0.72 m using equation (5) and $b_{\Delta T}$ = 0.22 m using equation (11). There is quite a large difference in the results obtained by these equations. The reason for this discrepancy is not clear. The reason may be partly explained by the large difference in the experimental set-up. The four steel towers used for equation (5) were only 1.8 m high, whereas the rack storage used here was 5.2 m high. The fire source and the combustible materials also differ. This discrepancy can be investigated further by using CFD models.

5.5 Heat release rate

The initial fire spread in rack storage fires can be divided into three distinct periods of time:

- The incipient period – *"incubation"* period
- The fast upward fire spread period – *"take-off"* period
- The horizontal fire spread period – *"eating-in"* period

The incipient period can vary considerably in time. It will depend on the size of the ignition source, the width of the flue space and the construction and type of the packaging material and the goods adjacent to the ignition source. This period can be named as the 'incubation' period, and is the time from ignition until the flames start to penetrate into the goods and the fire starts to propagate upwards. If there are no goods just behind the packaging material (e.g. wall of an empty box) the incubation time may be prolonged considerably.

The fast upward fire spread period follows directly after the incubation period. It can be regarded as the 'take-off' period of the upward fire spread. During this period, the flames start to spread rapidly upwards. This period is usually shorter than the incubation period. Accompanying the fast upward flame spread, we have a slow lateral flame spread on the vertical surfaces within the flues. At the same time we start to see flames penetrate into the horizontal flues (the horizontal gap between the stored boxes). The short horizontal flames will preheat the packaging material on the top and the bottom of the stored boxes. The length of the take-off period will depend mainly on the thermal properties of the packaging material, the height of the rack, the fire penetration rate at the ignition area and the width of the vertical flues. By definition, this period ends when the vertical pyrolysis zone reaches the top of the rack storage.

When the pyrolysis zone reaches the top of the rack, we observe continuation of the lateral flame spread inside the rack. This is the beginning of the horizontal fire spread period or the 'eating-in' period. The fire eats its way into the commodity. At the same time, we start to observe flame spread within the horizontal flues. The bottoms and tops of the boxes ignite and gradually we see flames penetrate towards

the edge of the boxes. Meanwhile, the fire in the vertical flues continues to penetrate into the commodity, and the fire gradually spreads laterally all the way to the edge of the boxes. Finally, we start to see flames on the outer face of the stored boxes. If the fire load consists of four pallets at the bottom, as in the present study, the flames will start to spread upwards on the outer surface of the boxes higher than the first tier. If the fire load consists of more than four pallets at the bottom, we will see flames spread towards adjacent boxes. This period, the eating-in period, is probably the most hazardous period. We can see it on the heat release rate curves in Figure 2 as the fast rising part of the curve. This period is usually shorter than the incubation period, and longer than the take-off period.

Now we can explain the results of the measured HRR for the different flue widths in regard to the three different phases of fire growth. An interesting observation from figure 2 is that the different groups clearly become separated during the eating-in period. By using this definition, we can also explain why we are able to normalise the HRR with the height, H. During this period, the horizontal flame spread (on the vertical surfaces) is nearly equal in size at all tiers (two, three, four or five). Thus, if we normalise it to H, we will get about the same results per tier or H, as the take-off period has very low values of HRR in comparison with the eating-in period.

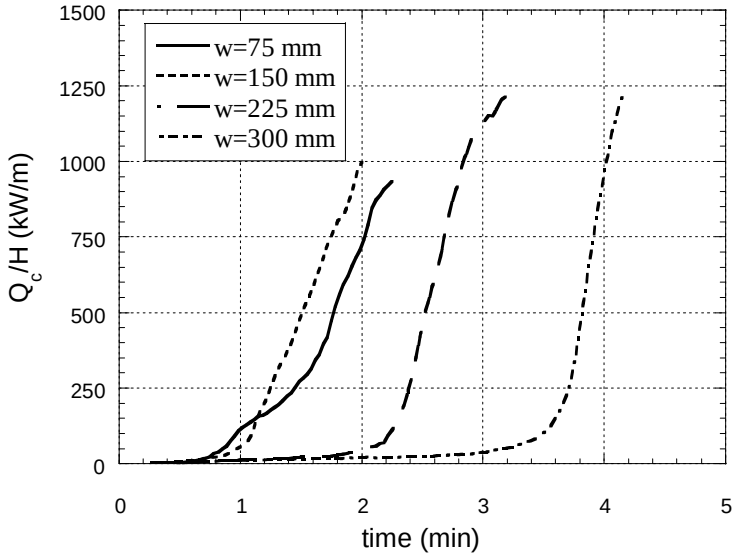

Figure 11 Convective HRR per height of the rack storage (H=5.2 m) measured by the Industry calorimeter for four different flue widths.

The measured convective HRRs per height of the storage tested (H=5.2 m) for the four different flue widths are presented in figure 11. It can be seen that the measured convective HRR per rack height is highly dependent on the flue width. Now we shall analysis the convective HRR curves by applying the definitions of the three time periods of fire growth.

It is apparent from the results shown in figure 11 that the incubation time is dependent on the flue width. This is also the case for take-off period. An indication of when the take-off period is about to end and the eating-in period is

about to start is when the flame tip reaches the top of the store. At this stage, the vertical pyrolysis zone is about 2/3 of the flame height. Shortly after the flame tip reaches the top, the pyrolysis zone will reach the top. The flame tip reached the top at different times, depending on the flue width: for w=75 mm it occurred at 0:41 min:sec, for w=150 mm; 0:58 min:sec, for w=225 mm; 2:10 min:sec and for w=300 mm; 3:39 min:sec. From figure 11, we can see that this occurs just before the heat release rate curves start to be directed slightly more upwards. If we assume that the incubation time is the time from ignition to the time when the flames clearly start to move upwards (defined here as the time when the flame height was 1.8 m on video), we get the following results: the incubation time for w=75 mm is 22 sec, for w=150 mm it is 28 sec, for w=225 mm it is 56 sec and for w=300 mm it is 2:00 min:sec. The difference between the times the flames reach the top of the rack storage and the incubation time is slightly less than the actual take off time (as defined here). For w=75 mm, the difference is 19 sec, for w=150 mm it is 30 sec, for w=225 mm it is 1:14 min:sec and for w=300m it is 1:33 min:sec. Consequently, we can conclude that the take-off time is also dependent on the flue width, w.

The slope of the curve during the eating-in period apparently increases with the flue width, w, for w $\geq$150 mm. The behaviour is somewhat different for w=75 mm, probably due to limited oxygen access into the flues, which slows down the fire growth rate. The reason for the increasing slope of the heat release curve with increased w (w$\geq$150 mm) is probably due to increased access to oxygen and increased mean beam length of the flames within the flues. This apparently influences the rate of the fire growth. If we compare figures 2 and 11, we see that for the same flue width, w=150 mm, we get similar results (see FMRC Class II). Thus we can conclude that the width of the vertical flue plays an important role in the fire growth rate of rack storage fires. The influence of the horizontal flues has not been considered in this study, but they may play an important role, especially in the later stage of the horizontal fire spread period.

Curve fits to the different heat release rates in figure 11 using the same type of equation as equation (9) yield curves which are quite close to the ones shown in figure 11. Here we assumed that the coefficient a in equation (9) is equal to 0.4 m. This corresponds to the width of the initial pyrolysis zone created by the four ignitions sources. Following fire growth constants were obtained for the different flue widths; (w=75 mm, α= 1.06 kW/m^2, β = 0.019 s^{-1} and b= 0.5 m/s; R=0.994), (w=150 mm, α= 1.16, β = 0.023 and b= 0.53 ; R=0.986), (w=225 mm, α=0.11 , β =0.041 and b=0.05 ; R=0.988) and (w=300 mm, , α= 0.003, β = 0.05 and b= 0.005 ; R=0.989). The derivation of the constants α, β , b is based on time in seconds. The reader must, however, be aware of the fact that the basic form of equation (9) was obtained by Ingason [25] for the vertical fire spread period (take-off period), which is only a part of the entire fire growth rate period. This was not fully understood by the author at the time equation (9) was developed. Why equation (9) works well for the entire fire growth period needs to be analysed further.

The author does not recommend that equation (9) should be used for HRRs above about 10 MW. The reason is that the data used in the analysis did not exceed 10 MW. In the case of four pallet loads at the bottom, as was tested in the present

study, the fire will proceed as long as there is material available (the eating-in period). But the rate of rise of the heat release curve will probably start to slow down and will gradually reach a maximum value before it starts to decay again due to lack of burning goods. In the case of more than four pallet loads at the bottom of the rack storage, the fire will spread to adjacent boxes and so influence the HRR curves. This is not considered in equation (9). Another important factor, which can influence the picture given here, is the ceiling height in relation to the rack height. When the flames reach to the ceiling, they will impinge on the ceiling and start to radiate towards the top of the adjacent boxes and row of racks. This will finally ignite the boxes on the top and the face of the boxes (high elevations) in adjacent row of racks.

5.6 The ratio of convective to chemical heat release rate

In the measurements of the HRR, we measured both the convective and the chemical HRR. Usually the convective HRR (Q_c) is about 70 % of the chemical HRR (Q). It is therefore of interest to investigate if this trend is similar for rack storage fires. Another interesting question is if this ratio is dependent on the flue widths.

The measured ratio of Q_c/Q is shown in figure 12. It is apparent that, at the initial stage of the fire, we have large heat losses to the walls of the boxes. This appears to be higher for the narrower flues. Figure 12 shows that, after about one minute into the test, the ratio approaches a value of 0.65 – 0.7 for all flue widths. For w=75 and 150 mm this occurs in the eating-in period of the fire growth, and for w=225 and 300 mm it occurs in the incubation period. It is obvious that, for the larger flue widths, the presence of the boxes does not have any great influence on the heat losses. This is obviously not the case for the narrower flues.

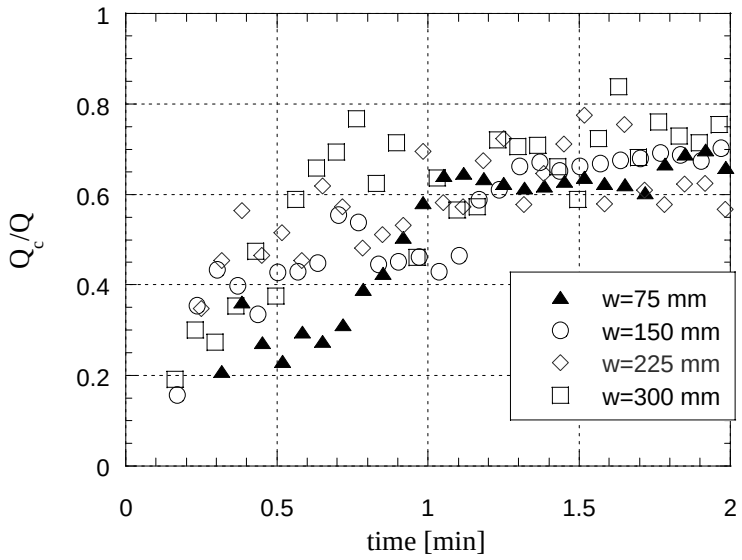

Figure 12 The ratio of convective HRR (Qc) to chemical HRR (Q) for different flue widths.

In order to analysis this in more detail, we have plotted the ratio of Q_c/Q as a function of the ratio of the flame height, L_f, to the rack height, H (figure 13). Thus, we can see more clearly that the narrower flues are more sensitive to the heat losses at the early stage of the fire. For the wider flues, this influence is almost negligible.

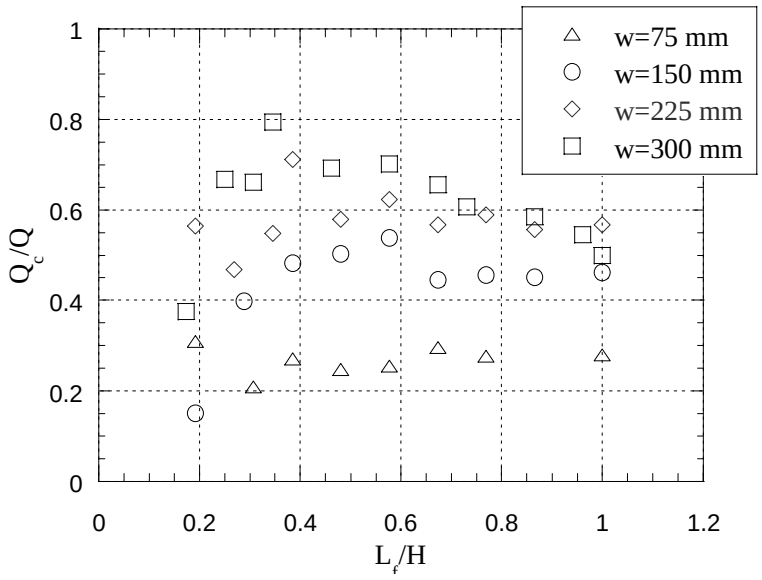

Figure 13 The ratio Q_c/Q plotted as a function of L_f/H for different flue widths.

5.7 Activation time of in-rack sprinklers

Table 1 shows the measured activation times of the in-rack sprinklers used in the tests. The in-rack sprinkler was of type Wormald A, Standard Spray Sprinkler (SSP), with an RTI value of 158 $m^{1/2}s^{1/2}$ (for the orientation used).

Table 1 The measured activation time in seconds of the in-rack sprinklers

	w=75 mm	**w=150 mm**	**w=225 mm**	**w=300 mm**
z=2.25 m	25	28	41	91
z=4.87 m	36	42	75	158

Now we are interested in simulating the activation time of the in-rack sprinklers using equation (10). The input to equation (10) can be obtained from equations (2)-(4) and (9). Equation (10) must be solved numerically, and the constants in equation (9) must be obtained from the experiments. Thus, we have made a curve fit of the experimental data for the actual time period using the same form as in equation (9). Then we use equations (2)-(4) as input into equation (10), using the Mathematica program [33]. The results are:

Table 2 The simulated activation time in seconds of the in-rack sprinklers using Mathematica [33].

	w=75 mm	**w=150 mm**	**w=225 mm**	**w=300 mm**
z=2.25 m	42	40	52	54
z=4.87 m	57	59	89	102

The results have been plotted in figures 14 and 15. There is a clear tendency for the simulated activation time to be higher than to the experimental results for w=75, 150 and 225 mm. The results are opposite to those for w=300 m.

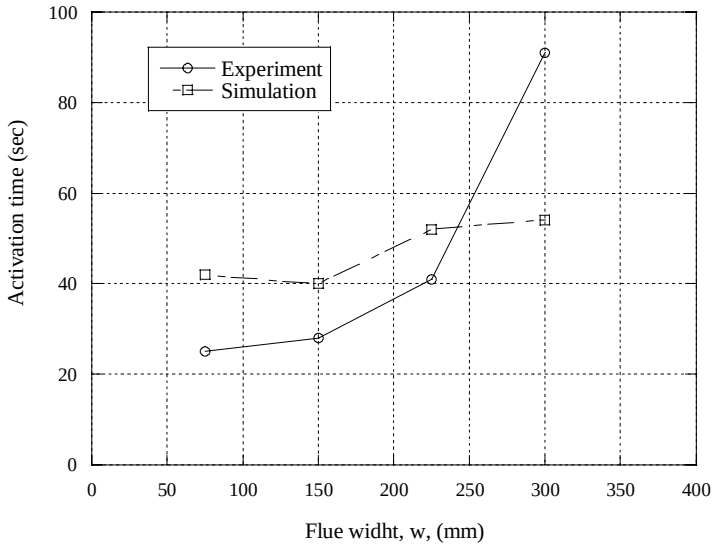

Figure 14 Comparison between measured and simulated activation time of in-rack sprinkler at z=2.25 m.

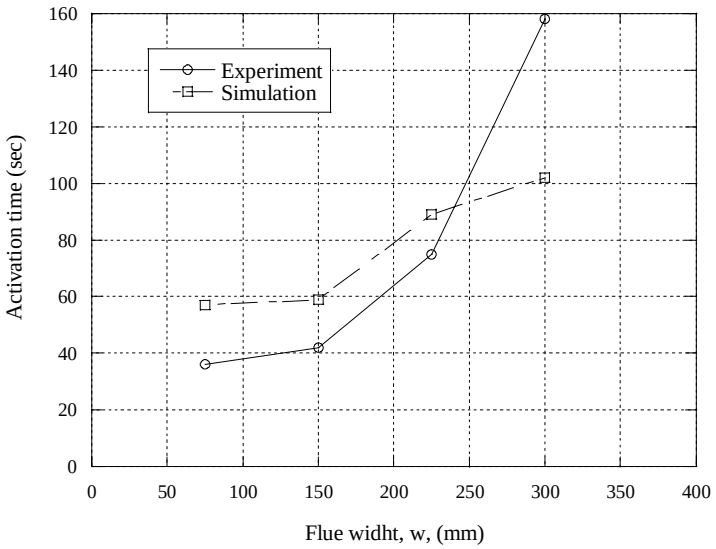

Figure 15 Comparison between measured and simulated activation time of in-rack sprinkler at z=4.87 m.

6 Conclusions

The aim of the study was to compare the results of four full-scale rack storage tests with the results of the 1:3 model-scale tests carried out in earlier studies [4, 5]. The width of the flues between the stacked Class II cartons was varied between 75 – 300 mm, while the height of the horizontal flue was kept constant at 300 mm. The in-rack flame height, the excess in-rack centreline gas temperature and the in-rack centreline gas velocity were plotted as functions of Q_c and z. The heat release rate and the off-centreline in-rack gas temperature were also plotted. Activation times of in-rack sprinklers are also presented.

The overall agreement between the full-scale tests and the earlier performed model scale tests was found to be reasonably good. There is a great scatter in the data, which was also the case in model case studies. The axi-symmetric power law correlations given for in-rack plume flow and flame heights did not fully correspond to the data obtained from experiments. The representation of the virtual source probably needs to be improved.

The experimental study presented here shows that the vertical flue space is an important parameter for the initial fire growth rate in the rack. Three distinct periods of fire growth were identified: the incubation period, the take-off period and the eating-in period. The last one is identified as the most hazardous period.

It was found that the narrower flues are more sensitive to heat losses to the boxes, especially at the early stage of the fire. For the wider flues, these losses were almost negligible. The average ratio of convective HRR to chemical heat release rate was found to be 0.67 for the time period between one and two minutes after ignition.

It was possible to predict the activation time of in-rack sprinklers at two different elevations by using the mathematical expressions given in the report. There is a tendency for the simulated activation time to be higher than to the experimental results for w=75, 150 and 225 mm. The results are opposite to those for w=300 m.

The results presented here are very encouraging and can be used for future development of flame spread and suppression modelling work.

7 References

1 Heskestad, G., *Engineering Relations for Fire Plumes*, Fire Safety Journal, 7 (1984) 25 - 32.

2 Alpert, R., *Turbulent Ceiling- Jet Induced by Large Scale Fires*, Combustion Science and Technology, 11, 197-213 (1975).

3 Beyler, C.L., *Fire Plumes and Ceiling Jets*, Fire Safety Journal, 11 (1988) 53-75.

4 Ingason, H., Experimental and Theoretical Study of Rack Storage Fires, PhD Thesis Lund University, Department of Fire Safety Engineering, Report LUTVDG/(TVBB-1013), 1996.

5 Ingason, H., Plume flow in high rack storages, Fire Safety Journal 36 (2001) p. 437 - 457.

6 Ingason, H., *In-Rack Fire Plumes*, Proceedings of the Fifth International Symposium on Fire Safety Science, Melbourne, Australia, 1997.

7 Yu, H-Z., and Kung, H-C., *Strong Buoyant Plumes of Growing Rack Storage Fires*, The Twentieth Symposium (International) on Combustion, P. 1567, The Combustion Institute, 1984.

8 Kung, H-C., Yu, H-Z, and Spaulding, R.D., *Ceiling Flows of Growing Rack Storage Fires*, Twenty-First Symposium (International) on Combustion, The Combustion Institute, PP. 121-128, 1986.

9 Yu, H-Z. and Stavrianidis, P., *The Transient Ceiling Flows of Growing Rack Storage Fires*, Fire Safety Science-Proceedings of the Third International Symposium, pp. 281-290.

10 Field, P., *Effective Sprinkler Protection for High Racked Storage*, Fire Surveyor, October 1985.

11 *Fire Tests on High-Piled Storage Protected by Automatic Sprinklers*, Comite Europeen des Assurances, TE 30153, April 1990.

12 Person, H., *Evaluation of the RDD-measuring Technique, RDD-tests of the CEA and FMRC standard plastic commodities*, Swedish National Testing and Research Institute, SP-Report 1991:04

13 Yao, C., *The Development of the ESFR Sprinkler System*, Fire Safety Journal, 14 (1988) pp. 65-73.

14 Troup, J., Protection of Warehous Retail Occupancies with Extra Large Orifice (ELO) Sprinklers, J. of Fire Prot. Engr. 8 (1), 1996, pp 1-12.

15 Troup, J., Extra Large Orifice (ELO) Sprinklers: An Overview of Full-Scale Fire test Prerformance, J. of Fire Prot. Engr. 9 (3), 1998, pp 27-39.

16 NFPA 231C, vol 6, National Fire Protection Association, Batterymarch Park, Quincy.

17 Heskestad, G., Flame Heights of Fuel Arrays with Combustion in Depth, Proceedings of the Fifth International Symposium on Fire Safety Science, Melbourne, Australia, 1997, p. 427-438.

18 Thomas, P.H., Some Comments on Fire Spread in High Racked Storage of Goods, Department of Fire Safety Engineering, Lund University, 1993.

19 Ingason, H., and DeRis, J., Flame Heat Transfer in Storage Geometries, Fire Safety Journal 31 (1998) 39-60.

20 Markstein, GH, Relationship between smoke point and radiant emission from buoyant turbulent and laminar diffusion flames, In. 20th Symp. On Combustion, The Combustion Institute, 1985, pp. 1055-1061.

21 Lee, S-L and Emmons, H.W., A Study of Natural Convection above a Line Fire, Journal of Fluid Mechanics, Vol. 11, part 3, p. 353-369.

22 McGrattan, K., Hamis, A., and Stroup, D., International Fire Sprinkler – Smoke & Heat Vent – Draft Curtain – Fire Test Project, Large Scale Experiments and Model Development, Technical Report, National Fire Protection Research Foundation, September 1998.

23 J.M.A Troup. Large-Scale Fire Tests of Rack Storaged Group A Plastics in Retail Operation Scenarios Protected by Extra Large Orifice (ELO) Sprinklers. Technical Report FMRC J.I. 0X1R0.RR, Factory Mutual Research Corporation.

24 Alvares, N., J., Hasegawa, H., Hout, K., Fernandez-Pello, A. and White, J., Analysis of a Runaway High Rack Storage Fire, Fire Safety Science-Proceedings of the Fourth International Symposium, pp. 1267-1278.

25 Ingason, H., Heat Release Rate of Rack Storage Fires, Proceedings of 9th Interflam 2001 Fire Science & Engineering Conference, Edinburgh 17-19th September 2001, p. 731-740.

26 Ingason, H. and Bror Persson, Numerical Simulation of the Wind Shadow Effect on the Convective Heat Transfer to Glass Bulb Sprinklers, Haukur, Fire Safety Journal 22 (1994) 329 - 340

27 Heskestad, G., and Smith, H.F., *Plunge Test for Determination of Sprinkler Sensitivity*, FMRC 3A1E2.RR, Factory Mutual Research Corporation, Norwood, Massachusetts, December 1980.

28 Heskestad, G. and Bill, R.B. Conduction Heat-Loss Effects on Thermal Response of Automatic Sprinklers, Factory Mutual Research Corporation, Norwood, Massachusetts, September 1987.

29 Dahlberg, m., The SP Industry Calorimeter, For rate of heat release rate measurements up to 10 MW, SP Report 1992:43.

30 Heskestad, G., A Fire Products Collector for Calorimetry into the MW Range, Report FMRC J.I. OC2E1.RA, Factory Mutual Research Corporation, Norwood.

31 McCaffrey, B.J. and Heskestad, G., A Robust Bi-directional Low-Velocity Probe for Flame and Fire Application, Combustion and Flame, 26, 125-127, 1976.

32 Ingason, H., Investigation of Thermal Response of Glass Bulb Sprinklers using Plunge and Ramp Tests, Fire Safety Journal 30 (1998) p. 71-93.

33 Mathematica, Version 4, Stephen Wolfram, The Mathematica Book, Fourth Edition, Wolfram Media/Cambridge University Press 1999.

SP Swedish National Testing and Research Institute
Box 857, SE-501 15 BORÅS, Sweden
Telephone: +46 33 16 50 00, Telefax: +46 33 13 55 02
E-mail: info@sp.se, Internet: www.sp.se

SP REPORT 2001:19
ISBN 91-7848-863-X
ISSN 0284-5172